Official journal of the JHL 2689-9620
www.light-am.com

Article Open Access

Two-photon photopolymerization directly initiated by spiropyran photochromic molecules

Dandan Ge[1], Jean Aubard[2], Erell Bodinier[1], Safi Jradi[1], Stéphanie Lau-Truong[2], Nordin Felidj[2], Renaud Bachelot[1] and Anne-Laure Baudrion[1,*]

Abstract

Here, we report the ability of spiropyrans to initiate two-photon polymerization (TPP) for the first time in the literature. The comparison and synergies between the spiropyran photochromic molecule of interest, namely 6-nitro-BIPS, and well-known photoinitiators of radical photopolymerization have been studied. The spiropyran (SPy) molecule can initiate TPP in the presence of trifunctional acrylic monomers and create true 3D structures. The comparison with Irgacure 819, a well-known Type-I photoinitiator, shows that SPy has a comparable capability for TPP. In addition, the combination of SPy with methyl diethanolamine increased the reactivity of both one- and two-photon polymerizations. In the last section, we discuss which SPy isomer is the active photochromic species capable of generating radicals for initiating two-photon polymerization.

Keywords: Spiropyran, Direct laser writing, Two-photon-photopolymerization, Photochromism

Introduction

The use of two-photon polymerization as a fast 3D printing technology has accelerated because of its application in photonic circuits[1], micro-electro-mechanical systems[2], biomedical devices[3,4], and many other medical and industrial areas[5–7]. The basic process of photopolymerization uses light as an energy source to induce the conversion of small unsaturated liquid monomers into solid polymers through polymerization reactions. The photoinitiator, quite sensitive to light irradiation, is excited via one-photon/two-photon absorption and forms the initiating species of radicals or cations to drive polymer chain growth[8]. Acrylate monomers are frequently used as radical-driven monomers for their efficiency in 3D photopolymerization[8]. In most cases, Norrish Type I or Norrish Type II photoinitiators are chosen to excite free-radical-driven photopolymerization[9]. The former can directly generate radical fragments under light irradiation. In contrast, the latter is a two-component photoinitiating system comprising an uncleavable sensitiser and a co-initiator, typically forming excited triplet states under light exposure and requiring a hydrogen donor to react[8–11]. Researchers are continuously looking for highly effective photoinitiators for different applications, such as titanocene[12], squaraine-based initiators[13], water-soluble ionic carbazole-based initiators[14], substituted thioxanthone-based photoinitiators[15], benzylidene cyclopentanones used for one/two-photopolymerization in visible light[16], pyrene-based initiators[17] that can work in the visible range with low light intensity, and hexanoylated ciprofloxacin[18] for biocompatible usage and many other highly sensitive

Correspondence: Anne-Laure Baudrion (anne_laure.baudrion@utt.fr)
[1]Light, nanomaterials, nanotechnologies (L2n) Laboratory, CNRS EMR7004, Université de Technologie de Troyes, 12 rue Marie Curie, 10004 Troyes Cedex, France
[2]Université Paris Cité, CNRS, ITODYS, F-75013 Paris, France

photoinitiators[19–21].

Photochromic molecules (PMs) have attracted considerable interest because of their reversible transformation between two isomers with different absorption spectra[16,17]. This optical switch leads to significant modifications in chemical or physical properties, depending on the PMs family[18,19]. Among them, spiropyrans (SPy), which show a switch between a colourless (transparent) isomer, SP (for spiropyran), and a coloured isomer, MC (for photomerocyanine), following absorption of UV/visible light[20], present outstanding changes not only in absorption spectra[21] but also in temperature[22], pH[23] and solvent polarity[24]. These characteristics make spiropyrans attractive for developing novel hybrid structures and materials.

Many studies have proposed to develop photochromic polymers, mainly by linking the photochromic groups to polymer monomers and building polymer backbones with branched photochromic groups[25–27]. Such photochromic polymers have proven their potential in optical switch applications[28], dynamic anti-counterfeiting marks[29], optical data storage and processing[30], and other more complex advanced integrated optical devices[31]. However, most studies on combining photochromic molecules and polymerization focus on the switch reaction. There are few studies on the direct interaction of photochromic molecules and monomers. Here, we demonstrated the ability of typical spiropyran molecules to initiate photopolymerization. The significance of our research is not only to discover new photoinitiators based on photochromic molecules, but also to deepen the understanding of the photochromic mechanism of spiropyran molecules in direct interaction with monomers.

Materials and Methods

Formulation preparation

In the spiropyran family, we chose for the present study, the 1′3′-Dihydro-1′,3′,3′-trimethyl-6-nitrospiro[2H-1-benzopyran-2,2′-(2H)-indole] (6-nitro-BIPS) because of its commercial availability. The other selected photochroms in the spiropyran family, namely, 6-Nitro-8-MeO-BIPS (indolino-6-nitro-8-methoxy-spirobenzopyran), 8-MeO-BIPS (indolino-8-methoxy-spirobenzopyran), the indolinospiro-naphthopyran (NAP) and a related indolinospiro-naphthooxazine (SPOX) have been chosen for comparison (the molecular structures of all these molecules are shown in Scheme 3 and will be discussed in the Results section). Both polymer monomers, pentaerythritol triacrylate (PETA) and trimethylolpropane triacrylate (TMPTA), as well as isopropylthioxanthone (ITX), N-methyl diethanolamine (MDEA, ⩾99%), were purchased from Sigma-Aldrich® and used as received.

The photopolymerisable formulation was a homogeneous mixture of monomer and photoinitiator:10 mg of 6-nitro-BIPS (SPy) powder was added to PETA under vigorous magnetic stirring to obtain a 2 g mixture containing 0.5 wt% SPy. In parallel, for comparison, 10 mg SPy powder and 200 mg MDEA were added into the PETA to get a 2 g mixture containing 0.5 wt% SPy + 10 wt% MDEA in PETA. The other formulations were prepared similarly. It takes 2 h for vigorous magnetic stirring to disperse SPy powder into PETA for the first time. Before each use, another 5 min of stirring was required to avoid precipitation.

Two-photon polymerization (TPP)

One drop of the photosensitive formulation, weighing approximately 10 mg, was directly pipetted onto a glass substrate. A commercial TPP direct laser writing system (Nanoscribe GmbH, Germany) was used to perform 3D microfabrication by two-photon polymerization (TPP). The 780 nm femtosecond laser was focused by an oil immersion objective (63x Zeiss, NA=1.4) onto the formulation droplet on the top surface of the glass substrate placed on an XYZ moving stage (a simple diagram is illustrated in Fig. S1). The laser power at the sample was calculated and controlled by the percentage of full power calibrated to 50 mW.

For threshold power measurement under different excitation wavelengths, a wavelength-tuneable femtosecond laser (Chameleon Ultra II) was used, and the laser was focused by an objective lens (40x0.6) to the substrate placed on the stage of an inverted microscope (IX71, Olympus). While maintaining the exposure time constant, the smallest laser power required to obtain the polymer dots was defined as the threshold power.

Observation by SEM

After polymerization, the sample was rinsed with acetone and isopropyl alcohol to remove the unpolymerized liquid. Scanning electron microscopy (SEM, Hitachi SU8030) was used to observe and analyse the morphology of the polymer microstructure. Au/Pd (3 nm) was deposited as a conductive layer on the sample before the SEM observation.

Photoluminescence measurement

A fluorescence confocal microscope (LSM780, Zeiss) was used to measure the fluorescence of the samples. A CW 561 nm laser was used to excite the sample through an x63 objective (1.4 NA), and the fluorescence was collected

through the same objective and sent to a GaAsP-PMT. A band-pass filter (from 604 nm to 674 nm) was used to collect the fluorescence signal.

Results

Two-photon polymerization

Direct laser writing (DLW) based on two-photon polymerization (TPP) is a mature method for fabricating 2D/3D microstructures and is also convenient for studying the TPP efficiency of different photoinitiators. The homogeneous solution of SPy powder dispersed directly in the PETA monomer has strong absorption in the UV region (< 400 nm), as shown in Fig. 1a (more information about the absorption measurements can be found in Fig. S2). After 30 s of UV irradiation, using a fibered and collimated light source (Hamamatsu, LC8 Lightingcure, equipped with a 150 W Hg/Xe lamp) through a UV band-pass filter (centred around 365 nm excitation wavelength), the solution of SPy in PETA displays an absorption band at 555 nm due to the photochromic transition. At the end of the UV irradiation, this visible absorption band decreased with time (*i.e.* the thermal fading process) to recover the state measured before UV irradiation. This photochromic reversible process has been widely studied for photochromic molecules[32,33]. Thus, all spiropyrans present absorption spectra in the UV range of 200–400 nm, with important absorption bands near 320–380 nm. Under UV irradiation, the C_{spiro}--O bond cleavage in SPy compounds leads to the formation of an "open form" coloured isomer called photomerocyanine (MC) as opposed to the "closed form" isomer which is colourless (transparent) and named spiropyran (SP) in the text for convenience. The "open form" isomer is named photomerocyanine because its transoid structure is quite similar to that of merocyanine dyes (see Scheme 1 below).

SPy absorption in UV makes it useful for two-photon absorption under 780 nm laser excitation[34]. The pristine solution exhibiting an absorption band at 555 nm, indicates that a small amount of the MC isomer is already present in the monomer solution without UV irradiation. For TPP experiments, it is important to note that the sensitivity of a formulation can be determined by fabricating polymer structures at different incident laser powers to find the minimum laser power (threshold) allowing the formation of a polymer structure. Comparing these thresholds for two different formulations indicates which one is the most sensitive, that is which one obtains the minimum threshold power. When using the formulation containing 0.5 wt% SPy in PETA, Fig. 1b shows the inverse of the threshold powers for triggering TPP under different wavelengths, which shows a decreasing trend from 680 to 900 nm. Fig. 1c shows the results of Fig. 1a and b for better visualisation. The normalised inverse square of the threshold power ($1/P^2$) under different wavelengths exhibits the same changing trend as the normalised absorption under half of the excitation wavelength. This provides good evidence of the two-photon process[35,36]. Fig. 1d, e, and f show examples of 1D polymer dots, a 2D polymer line array, and a 3D polymer woodpile fabricated by DLW with SPy photochromes diluted in PETA. This proves the ability of the SPy photochrome to induce TPP directly without any other additives (photoinitiator or co-initiator).

Polymerizability efficiency

To evaluate the efficiency of SPy (6-nitro-BIPS) in initiating TPP, we first compared the TPP results initiated by SPy with a well-known Norrish Type I photoinitiator

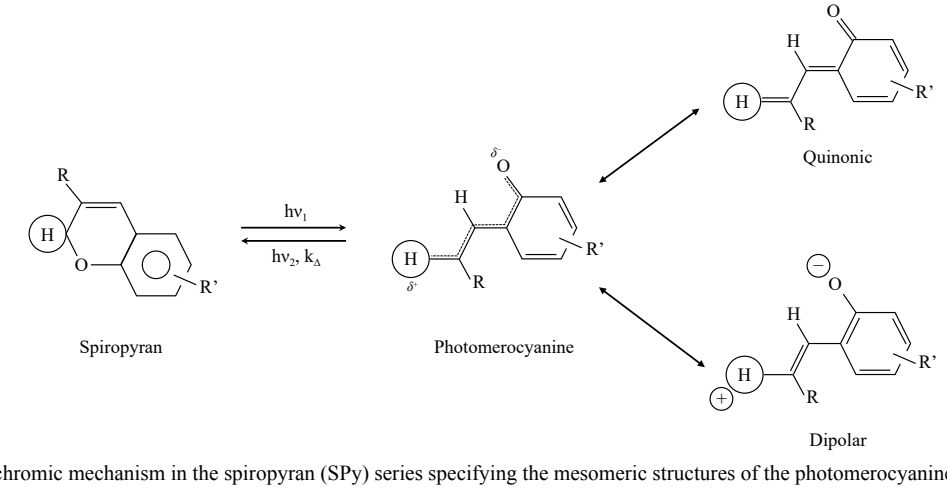

Scheme 1 Photochromic mechanism in the spiropyran (SPy) series specifying the mesomeric structures of the photomerocyanine (MC) form.

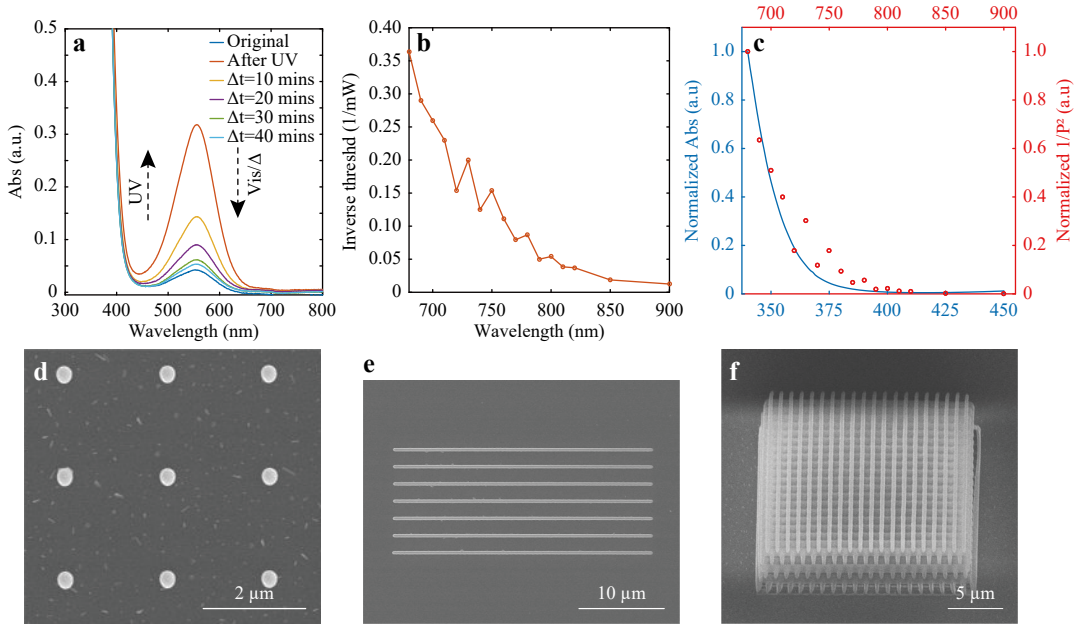

Fig. 1 a Absorption spectra of 0.0125 wt% SPy dissolved in PETA before (blue line) and after 30 s UV irradiation (orange line). The absorption spectra between these two curves corresponds to measurements performed within decades of minutes after stopping UV irradiation. **b** Inverse of the threshold powers (smallest laser powers needed to trigger TPP) plotted as a function of the excitation wavelengths (the exposure time is kept constant at 60 ms.) **c** Normalised absorption of SPy in PETA (in blue) and normalised square of the inverse threshold laser power (in red) as a function of the illumination wavelength. **d** Polymer dots, **e** polymer lines, and **f** polymer woodpile fabricated by TPP. Curing laser is 780 nm. **b** to **f** use the solution of 0.5 wt% SPy in PETA.

Irgacure 819 (IRG819), whose absorption spectrum is shown in Fig. S3. Even if IRG819 presents a low two-photon-absorption cross section[37], it is commercially available and inexpensive. We fabricated polymer lines, as depicted in Fig. 1e and measured their width in the SEM images. Fig. 2a shows the polymer line widths obtained with different laser powers for fabrication. 0.5 wt% SPy in the PETA monomer presented comparable performance to the formulation of 1 wt% IRG 819 in the same monomer. In particular, the smallest laser power for obtaining visible polymer lines for the former formulation was slightly lower. When these two components, 0.5 wt% SPy and 1 wt% IRG 819, were added together to PETA, the result of their joint action was better than the effect of each of them alone and just equal to the results of 1 wt% SPy in PETA, as shown in Fig. 2a. IRG 819 is known as a Norrish Type I radical-free photoinitiator[38]. The result of Fig. 2a suggests that SPy and IRG819 can work together to obtain a superimposed effect. This interaction is poorly understood and will be the subject of further investigation.

To understand the behaviour of SPy as a photoinitiator, it was compared with 2-isopropylthioxanthone (ITX), a well-known Norrish Type-II photoinitiator[37]. The absorption spectra are shown in Fig. S3. This kind of photoreaction requires a co-initiator to provide hydrogen for polymerization[9,39] and we chose MDEA as it is one of the most common co-initiators[40–42]. In Fig. 2b, a formulation made with 1 wt% ITX in PETA (light-green curve) shows a very low sensitivity compared to the one made with 0.5 wt% SPy (light-blue curve). In contrast, it becomes much more sensitive after adding 10 wt% MDEA to both formulations (dark-blue and dark-green curves, respectively). Indeed, the threshold laser power for getting a polymer line decreases five times (from 25% to 5% between the green curves), and the line width using the same laser power presents a large increase (at 30% of laser power, adding MDEA increases the line width from 135 nm to 780 nm). For SPy, adding 10 wt% MDEA led to the same behaviour but with the smallest importance. Indeed, the threshold power goes only from 17.5% to 10% (1.75 times smaller), and the line width obtained using a 30% laser power increases from 260 nm to 393 nm.

In the case of SPy (the 6-nitro-BIPS in particular), it must be considered that this compound is commonly used as a photoacid and enables protonated E to Z isomerisation under certain conditions[20]. Thus, upon UV irradiation, the open-form photomerocyanine with a charged dipolar electronic configuration (dipolar form in Scheme 1), characteristic of 6' nitro-substituted spiropyrans, presents a negatively charged oxygen with a higher affinity for the

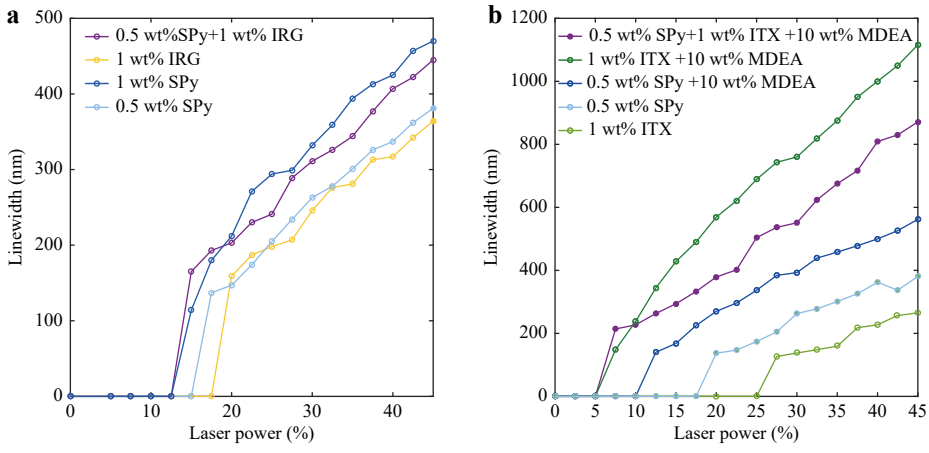

Fig. 2 a Comparison of the line widths of polymer lines obtained using Irgacure 819 or SPy as initiators in PETA. **b** Comparison of the line widths of polymer lines obtained using isopropylthioxanthone (ITX) or SPy as initiators in PETA with or without the co-initiator MDEA. The scan speed is set to 500 µm/s. Typical error bars are shown in Fig. S4.

proton than the closed-form isomer, spiropyran. This dipolar MC can carry out proton uptake, leading to protonated trans-photomerocyanine (see Scheme 16 in Ref. 20). This behaviour may be similar to that of a Type-II initiator, which takes a hydrogen atom from the co-initiator.

When 0.5 wt% SPy is present with 1 wt% ITX and 10 wt% MDEA (purple curve in Fig. 2b), the power threshold for starting polymerization is almost unchanged compared to 1 wt% ITX + 10 wt% MDEA (in dark green). However, when the laser power exceeded the threshold, the polymer line width obtained by the former did not increase as expected. As shown in Fig. 2b, the polymer line widths obtained using 0.5 wt% SPy+1 wt% ITX +10 wt% MDEA (in purple) are bigger than those using 0.5 wt% SPy + 10 wt% MDEA (in dark-blue) but less than using 1 wt% ITX +10 wt% MDEA (in dark-green). Regardless of the laser power or scan speed, no shaped polymer lines can be fabricated with only PETA monomers or a mixture of PETA and MDEA (see. Fig. S5).

To investigate the influence of MDEA on the reactivity of SPy in photopolymerization, different concentrations of MDEA were added into the original formulations of 1 wt% ITX (Fig. 3a) and 0.5 wt% SPy (Fig. 3b) in PETA, and their polymerization sensitivity was checked by measuring the width of the obtained polymer lines by SEM. At a given laser power, adding MDEA significantly increased the polymer line widths. Moreover, adding the MDEA decreased the laser threshold power for both formulations. However, the sensitivity of the ITX formulations was higher than that of the SPy formulations, as the obtained line widths were larger and the threshold powers were lower. Finally, for both formulations, saturation behaviour is reached after a certain concentration of MDEA. However, this saturation is reached very quickly for SPy as only 2.5 wt% MDEA is sufficient to observe the saturation.

The change in the TPP curve of ITX in the presence of MDEA corresponds to the behaviour of a Norrish Type-II initiator. However, the TPP sensitivity of SPy, which increases after adding MDEA, seems to be independent of the concentration of this latter molecule. Indeed, fluorescence quenching measurements of SPy dissolved in acetonitrile did not show any decrease in the fluorescence intensity in the presence of MDEA (Fig. S6a). This result indicates that MDEA does not quench the SPy excited state, which is not typical behaviour of the Norrish Type II initiator. In contrast, the fluorescence intensity increased with increasing MDEA concentration. This behaviour led us to conclude that MDEA favours the formation of the MC isomer. The absorbance spectra of SPy in acetonitrile in the presence of MDEA (Fig. S6b) confirms this conclusion, even showing the formation of MC dimers at high concentrations.

The influence of MDEA was also investigated during one-photon polymerization. For this, infrared spectroscopy was used to monitor the C=C bond at 810 cm^{-1} at different UV irradiation times of 2 different formulations (0.5 wt% SPy/PETA and 0.5 wt% SPy/5 wt% MDEA/PETA). The results presented in Fig. S7 show that MDEA makes the photopolymerization faster and increases the monomer conversion rate (25% without MDEA vs 35% with MDEA). This behaviour is consistent with the results observed for TPP.

For a better comparison of all prepared formulations, Fig. 4 lists the effective working window of each formulation. The working window is defined as the

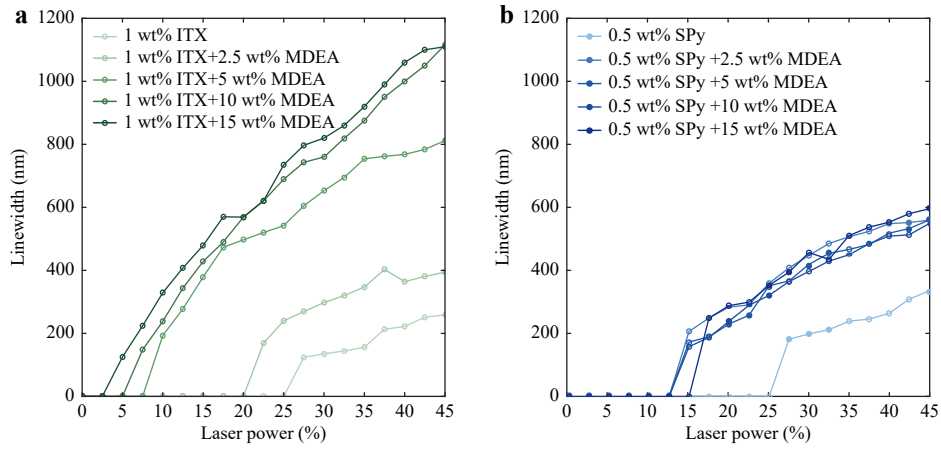

Fig. 3 Line widths of polymer lines as a function of the incident laser power using a formulation of **a** 1 wt% ITX and **b** 0.5 wt% SPy in PETA mixed with different concentrations of MDEA. The scan speed is set to 500 μm/s for all measurements.

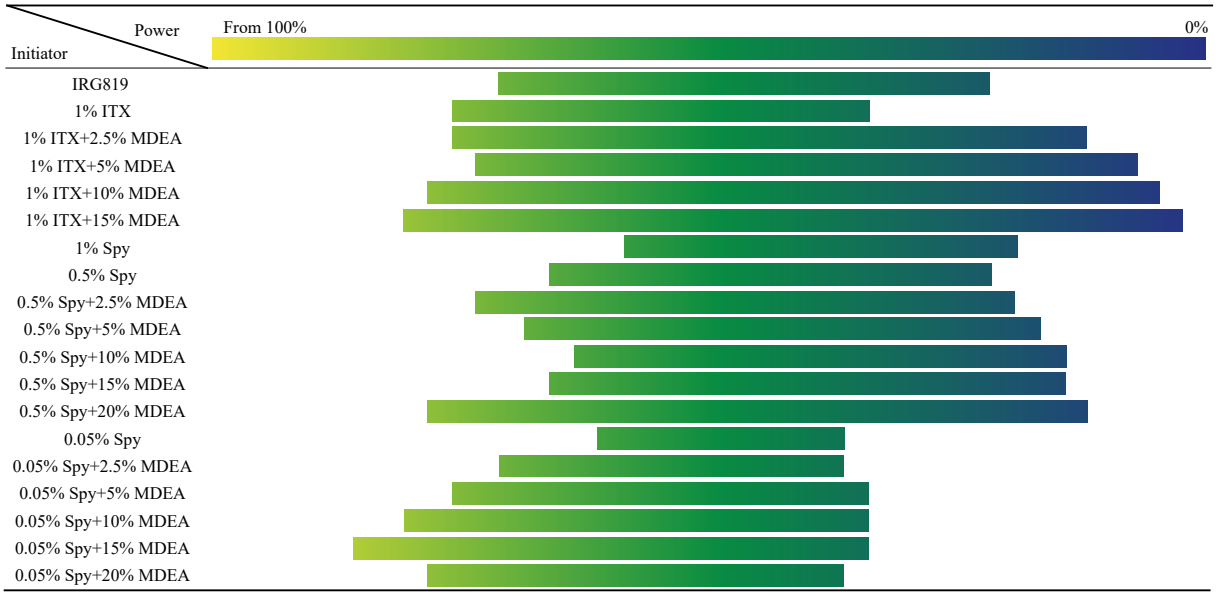

Fig. 4 The laser power working windows of different formulations, measured by SEM on TPP fabricated polymer lines at different laser powers. The scan speed has been fixed at 500 μm/s.

effective power window that can be used to fabricate polymer lines. Below this power window, no polymer can be printed, and above this window, an overheating explosion at the laser focus occurs. As shown in Fig. 4, adding MDEA to any formulation extends the power working window. The concentration of SPy alone in PETA seems to play an important role in the power working window as 0.5 wt% increases it compared to 0.05 wt%, but also compared to 1 wt%.

Moreover, 0.5 wt% SPy in PETA has a slightly larger power working window than the 1 wt% ITX in PETA. However, after adding 2.5 wt% MDEA to both formulations, the working window of the formulation containing 1 wt% ITX was widened, while the expansion of the working window of 0.5 wt% SPy was smaller. Adding 20 wt% MDEA to a 0.5 wt% SPy solution has the largest working window, but it is slightly narrower than the formulation of 1 wt% ITX with 15 wt% MDEA. These results show that SPy alone can initiate TPP. Moreover, cooperation with MDEA can lead to interesting efficiency in the TPP process. The molecular interactions involved in this process are still under investigation.

Photochromic switch ability

To characterise the ability of the fabricated photochromic polymer 3D structures to switch from one

isomer to another, standard UV-visible absorption spectra could not be obtained because of the micrometric size of the structures. Fortunately, after UV irradiation, the SP isomer transforms into the MC isomer, which emits fluorescence[43,20]. Thus, this fluorescence emission can be used to characterise the photochromic ability of locally built polymer structures. Hence, a micro-square with a size of 100 × 100 × 0.5 µm was fabricated by TPP using a formulation of 0.5 wt% SPy in PETA monomer. The fluorescence from this square immediately after fabrication is shown in Fig. 5a. This fluorescence signal originates from the MC isomers already present before UV irradiation. The distribution of the fluorescence intensity per pixel before and after UV irradiation (Fig. 5b) shows that no increase in fluorescence intensity can be observed.

In contrast, the fluorescence intensity weakly decreased after UV irradiation, indicating MC's photo-bleaching. We attempted to add MDEA to the previous solution. However, the fluorescence analysis from the obtained micro-squares before and after UV irradiation (Fig. 5c) showed no remaining photochromic behaviour.

As the TPP process seems to inhibit the photochromic transition and considering the MC isomers as the reactive species, the first hypothesis concerns the damage to the molecules because of the high local laser density during the fabrication process. Indeed, the photodegradation of MC under strong UV irradiation is a well-known side reaction in nitro-substituted spiropyrans[43]. If the number of MC isomers decreases during photopolymerization, the SP-MC isomerisation equilibrium is displaced toward creating MC isomers; therefore, the concentration of SP isomers decreases. If some SP isomer remains in the polymer, another hypothesis explaining why it does not experience photochromic transition concerns the steric repulsion caused by the polymer environment. Indeed, many studies have demonstrated that the switch function of spiropyrans is restricted in the solid state[22]. For 6-nitro-BIPS, molecules mixed inside the formulation should be trapped in the cross-linked net of the polymer after polymerization, and the photochromic behaviour, originating from photoisomerisation, may be inhibited because of the lack of free space inside the polymer net.

Therefore, to better understand the process, it is necessary to investigate whether the SP isomer remains in the photopolymer after fabrication. The pristine SPy solutions we used were, under our experimental conditions and before UV irradiation, mixtures of SP and MC isomers, as indicated by the presence of an absorption band around 555 nm, characteristic of the MC isomer (purple and blue lines in Fig. 6a). This phenomenon is related to solvatochromism[44]. Indeed, in the present experiments, a progressive pink colouration of 6-nitro-BIPS solutions was observed with increasing solvent polarity without any UV irradiation. This is due to the important polar character of the 6-nitro-BIPS-MC isomer, stabilised in its dipolar form in polar solvents[44]. In this case, ring opening can occur without UV irradiation through electrostatic cleavage of the C-O bond and is accompanied by a blue shift characteristic of a negative solvatochromism[44]. Therefore, MC isomers were already present in the pristine solution. The amount of the MC isomer depends on the polarity of the solvent. Therefore, we compared the previous formulation with a new formulation composed of a different monomer. In addition to PETA, which has a side chain composed of a hydroxyl group leading to high polarity, trimethylolpropane triacrylate (TMPTA) is another monomer in which the hydroxyl group is replaced by a methyl group, thus leading to a lower polarity and a concomitant decrease in the amount of the MC isomer in the mixture.

Fig. 6a displays the absorption spectra of both formulations (SPy in PETA and TMPTA), taking the

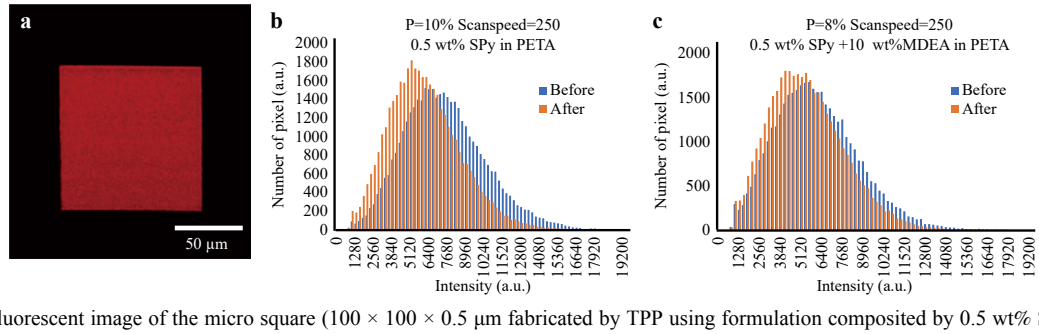

Fig. 5 a A fluorescent image of the micro square (100 × 100 × 0.5 µm fabricated by TPP using formulation composited by 0.5 wt% SPy in PETA monomer, using a scan speed of 250 µm/s and a laser power of 10%. **b** Statistical graph of fluorescence intensity distribution per number of pixels obtained from (a) before and after the photochromic transition. **c** Statistical graph of fluorescence intensity distribution from the micro square fabricated using a formulation of 0.5 wt% SPy + 10 wt% MDEA in PETA.

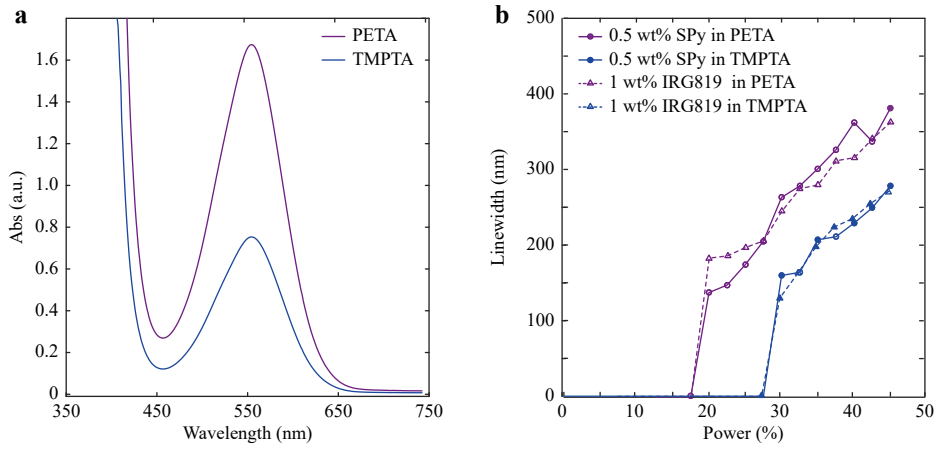

Fig. 6 a Absorption spectrum of 0.5 wt% SPy dissolved in PETA (purple line) and TMPTA (blue line). **b** Line widths of polymer lines as a function of the incident laser power used on formulations of 0.5 wt% SPy and 1 wt% IRG819 in PETA or TMPTA separately. The scan seep is set to 500 μm/s.

monomer's absorption as a reference. It clearly shows that there is more MC isomer in PETA than in TMPTA, as the 555 nm absorption band is higher for PETA than TMPTA. We then fabricated polymer lines by TPP with both formulations and varying laser power. Fig. 6b shows the line widths of the fabricated polymer lines as a function of the incident laser power for both formulations (see solid lines). It clearly shows that the power threshold of PETA solution containing 0.5 wt% SPy is lower than that of TMPTA solution containing the same concentration of SPy.

Moreover, under the same laser power, bigger polymer line widths are obtained using PETA, compared to TMPTA, leading us to conclude that the formulation with PETA is more photosensitive than the one with TMPTA. A first hypothesis might be that this higher sensitivity comes from the larger amount of MC isomer in the formulation. We thus used IRG819 as a reference and obtained the same sensitivity difference as for SPy. This difference in sensitivity could come from the monomer itself, and it does not allow us to conclude directly on the TPP ability of the MC isomer in different monomers.

To further understand the photopolymerization process, it is necessary to compare the different photochromes diluted in PETA. To choose relevant photochromic molecules, we need to consider the electronic configuration of the MC forms, which depends on both the molecular (chemical) structure and polarity of the solvent (medium). Thus, for the nitro-substituted SPy (those with a nitro group at position 6', see Scheme 2 below), for all photomerocyanines in this series, the electronic distribution has a dipolar (zwitterionic) character, showing a negative solvatochromism (i.e. absorption spectra show a blue shift

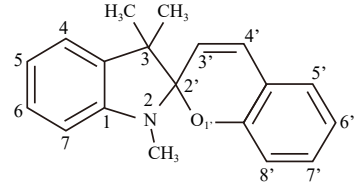

Scheme 2 General chemical structure of indolinospirobenzopyran family

with increasing polarity of the solvent) and are stabilised by polar solvents[44].

Although the most stable photomerocyanine isomers obtained from UV irradiation of SPy in this series are those with a nitro group at position 6' and a methoxy group at position 8' (Scheme 2), for practical reasons, 6-nitro-BIPS, which is commercially available, is the most often used. In contrast to these extensively studied nitro-substituted spiropyrans, in which negative solvatochromism was observed for the photomerocyanines[44], for indolinospironaphthopyrans and other indolinospirobenzopyrans without a nitro substituent, and for related spirooxazines, positive solvatochromism was observed for the MC photomerocyanines[45] (the absorption spectra of MC showed a red-shift when going from non-polar to polar solvents). This indicates that for these spiropyran compounds, the electronic distribution within the MC isomer mainly leads to an apolar quinoidal structure (see Scheme 1, quinonic form), in contrast to the photomerocyanines of nitro-substituted spiropyrans, in which the structure is essentially dipolar. Similarly, the photochromic behaviour of indolinospiro-naphthooxazines was similar to that of indolinospiro-naphthopyrans and other non-nitro-substituted spiropyrans[45].

Therefore, supplementary experiments in two-photon photopolymerization (TPP) were performed using a set of selected photochromes in the spiropyran (SPy) family, namely, 6-Nitro-8-MeO-BIPS (indolino-6-nitro-8-methoxy-spirobenzopyran), 8-MeO-BIPS (indolino-8-methoxy-spirobenzopyran), indolinospiro-naphthopyran (NAP), and a related indolinospiro-naphthooxazine (SPOX), the structures of which are shown in Scheme 3.

We also performed solvent-dependence experiments with the same photochromes (including 6-nitro-BIPS) to check the solvatochromism of SPy and SPOX. The results of the solvatochromism experiments are shown in Fig. 7 for 6-nitro-BIPS and in Fig. S6 for the other photochromes. The absorption spectra of MC (obtained after 1-mn, 365-nm UV irradiation) for the nitro-substituted spiropyrans, *i.e.,* 6-Nitro-BIPS and 6-Nitro-8-MeO-BIPS, show hypsochromic (blue) shifts with increasing solvent polarity; see, for example, the blue shift from toluene (apolar) to ethanol (polar) in Fig. 7. Naphthopyran (NAP), 8-MeO-BIPS, and spirooxazine (SPOX) show, as expected, a reverse behaviour and a bathochromic (red) shift with increasing solvent polarity[44,45] (Fig. S8). The two nitro-substituted spiropyrans are coloured in polar solutions, light red for 6-nitro-BIPS, and deep blue for 6-Nitro-8-MeO-BIPS, indicating a significant amount of MC in the pristine SPy solution, *i.e.,* without UV irradiation. In contrast, 8-MeO-BIPS, NAP, and SPOX were less coloured in ethanol.

TPP experiments were performed using the set of the above four photochromic molecules (Figs. S9–S12). The molecules were mixed with PETA or PETA and MDEA, and we fabricated polymer lines using the same process as described above for 6-nitro-BIPS (SPy). From these experiments, it appears that 6-Nitro-8-MeO-BIPS can initiate two-photon polymerization very efficiently because 0.5 wt% 6-Nitro-8-MeO-BIPS in PETA has the same effect (even better) as 0.5 wt% SPy (6-nitro-BIPS) in PETA (see Fig. S11). In contrast, 8-MeO-BIPS and NAP did not initiate two-photon polymerization (see Fig. S9 and S12). Finally, 0.5 wt% SPOX seems to initiate two-photon polymerization but with very poor efficiency. (Fig. S10).

These results show an evident correlation between the efficiency of TPP initiation and the presence of dipolar (zwitterionic) MC isomers stabilised in polar mixtures and arose specifically from nitro-substituted spiropyrans. On the contrary, for formulations containing 8-MeO-BIPS, and NAP for which MC isomers are endowed mainly with an apolar quinonic form and are not (or weakly) present in PETA polar medium, these spiropyrans without a nitro substituent cannot initiate TPP. Furthermore, this work demonstrates that if the nitro-substitution on the benzopyran moiety of the molecule markedly enhances MC photomerocyanine formation with a dipolar (zwitterionic) character and increases the TPP efficiency, it unfortunately favours the disappearance of the SP isomer owing to a degradation reaction through an efficient photooxidation process of the so-formed MC isomers[44,46], leading to the loss of photochromism during the two-photon polymerization process. Although the exact nature of the oxidation steps is not precisely known, it was proposed that the photooxidation mechanism would result, at least in part, from the interaction of the biradical form of MC with molecular oxygen under UV irradiation[46]. Electronic Spin Resonance (ESR) spectroscopic studies have proven the existence of these biradicals in solutions of photochromic molecules (including SPy and SPOX) during irradiation[47]. Moreover, the authors argued that these biradical species arise from the homolytic cleavage of the C_{spiro}--O bond, and their interaction with molecular oxygen leads to photodegradation products[47]. These highly reactive

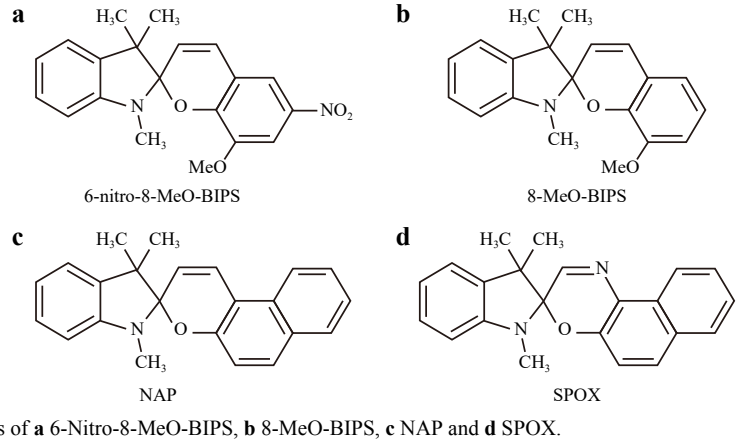

Scheme 3 Chemical structures of **a** 6-Nitro-8-MeO-BIPS, **b** 8-MeO-BIPS, **c** NAP and **d** SPOX.

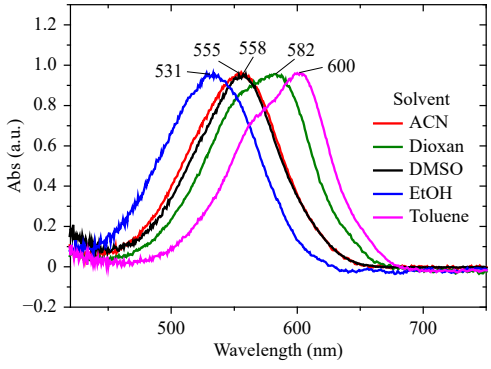

Fig. 7 Absorption spectra of 6-nitro-BIPS in different solvents at room temperature, obtained after UV irradiation at 365 nm.

radicals under TPP conditions likely favours monomer photopolymerization.

In conclusion, we can now establish a scale of efficiency for various spiropyrans used to initiate two-photon-photopolymerization. The following order was obtained:6-nitro-8-MeO-BIPS ⩾ 6-nitro-BIPS > 8-MeO-BIPS and NAP. Thus, 6-nitro-BIPS, which is commercially available, is the best candidate for further experiments using nitro-substituted spiropyrans as photoinitiators of polymerization. However, the reactivity of photoinitiators is related to many parameters, such as the ability of the photoinitiator to absorb light (absorption cross-section), its ability to generate reactive species, and the reactivity of these species toward monomer C=C bonds. By comparing different photochromic molecules, we attempted to find a correlation between photosensitivity and the number of MC isomers. Thus, by comparing the photosensitivity of different photochromic molecules, we should consider the fact that the number of absorbed photons and/or the number of generated radicals and/or the reactivity of these radicals toward the C=C bonds might be different. By concluding that higher amounts of MC isomers absorb more light and generate more radicals, one could consider that these radicals come, at least in part, from the photooxidation of MC isomer[47] (i.e. from the degradation process). Further studies are underway to confirm this hypothesis.

Conclusion

This study mainly discusses the ability of spiropyrans to function as photoinitiators for two-photon-photopolymerization. Nitro-substituted spiropyrans alone can initiate the photopolymerization of acrylate monomers with interesting efficiency. Adding a co-initiator as a hydrogen donor can improve the photosensitivity of a formulation composed of 6-nitro-BIPS spiropyran and polymer monomers and decrease the threshold power for photopolymerization. This co-initiator seems to increase the amount of the MC isomer in the formulation without influencing the excited state of the photo-initiator, contrary to its typical behaviour with Type II initiators. The 6-nitro-BIPS photochrome in polar monomers showed interesting sensitivity for initiating two-photon polymerization. This ability seems to arise from the photomerocyanine isomer presenting a dipolar character. Unfortunately, it results in the disappearance of the spiropyran isomer, leading to the loss of photochromism during the two-photon polymerization process. New experiments involving other photochromic molecules, such as certain spirooxazine derivatives, which present much better fatigue resistance than spiropyran derivatives[44], could lead to the conservation of the photochromic ability within the photopolymer.

Acknowledgements

DG and AB acknowledge the region Grand-Est and FEDER funds for their support through a postdoctoral fellowship. This work was conducted within the framework of the Graduate School NANO-PHOT (École Universitaire de Recherche, contract ANR-18-EURE-0013). J. A. would like to thank Prof. Robert Guglielmetti, missed by all since 2018, whose contribution to the field of photochromic molecules and materials is internationally recognised. R. Guglielmetti and his co-workers developed for more than 30 years the design and synthesis of a broad range of photochromic systems such as spiropyran, spirooxazine and chromene derivatives. Some of the selected spiropyrans used here were the fruits of several years of collaboration.

Author contributions

AB directed the project; DG, SL, J. A., and EB performed the experiments. D.G., A.B., J.A., S.J., R.B., and N.F. analysed the experimental results. All authors contributed to the discussion and preparation of this paper.

Conflict of interest

The authors declare no competing interests.

Supplementary information is available for this paper at https://doi.org/10.37188/lam.2023.004.

Received: 06 September 2022 Revised: 20 January 2023 Accepted: 20 January 2023

Accepted article preview online: 20 January 2023

Published online: 24 March 2023

References

1. Moughames, J. et al. 3D printed multimode-splitters for photonic interconnects. *Optical Materials Express* **10**, 2952-2961 (2020).
2. Ulkir, O. Design and fabrication of an electrothermal MEMS micro-actuator with 3D printing technology. *Materials Research Express* **7**, 075015 (2020).
3. Li, J. H. et al. 3D printing of hydrogels: rational design strategies and emerging biomedical applications. *Materials Science and Engineering: R: Reports* **140**, 100543 (2020).
4. Derakhshanfar, S. et al. 3D bioprinting for biomedical devices and

tissue engineering: A review of recent trends and advances. *Bioactive Materials* **3**, 144-156 (2018).
5. Ngo, T. D. et al. Additive manufacturing (3D printing): A review of materials, methods, applications and challenges. *Composites Part B:Engineering* **143**, 172-196 (2018).
6. Liaw, C. Y. & Guvendiren, M. Current and emerging applications of 3D printing in medicine. *Biofabrication* **9**, 024102 (2017).
7. Bikas, H., Stavropoulos, P. & Chryssolouris, G. Additive manufacturing methods and modelling approaches: a critical review. *The International Journal of Advanced Manufacturing Technology* **83**, 389-405 (2016).
8. Bagheri, A. & Jin, J. Y. Photopolymerization in 3D printing. *ACS Applied Polymer Materials* **1**, 593-611 (2019).
9. Marchetti, B., Karsili, T. N. V. & Ashfold, M. N. R. Exploring Norrish type I and type II reactions: an *ab initio* mechanistic study highlighting singlet-state mediated chemistry. *Physical Chemistry Chemical Physics* **21**, 14418-14428 (2019).
10. Green, W. A. Industrial Photoinitiators: A Technical Guide. (Boca Raton: CRC Press, 2010).
11. Ligon, S. C. et al. Polymers for 3D printing and customized additive manufacturing. *Chemical Reviews* **117**, 10212-10290 (2017).
12. Kitano, H. et al. Unexpected visible-light-induced free radical photopolymerization at low light intensity and high viscosity using a titanocene photoinitiator. *Journal of Applied Polymer Science* **128**, 611-618 (2013).
13. Giacoletto, N., Ibrahim-Ouali, M. & Dumur, F. Recent advances on squaraine-based photoinitiators of polymerization. *European Polymer Journal* **150**, 110427 (2021).
14. Dumur, F. Recent advances on pyrene-based photoinitiators of polymerization. *European Polymer Journal* **126**, 109564 (2020).
15. Noirbent, G. & Dumur, F. Photoinitiators of polymerization with reduced environmental impact: nature as an unlimited and renewable source of dyes. *European Polymer Journal* **142**, 110109 (2021).
16. Barachevsky, V. A. Advances in photonics of organic photochromism. *Journal of Photochemistry and Photobiology A:Chemistry* **354**, 61-69 (2018).
17. Zhang, J. J., Zou, Q. & Tian, H. Photochromic materials: more than meets the eye. *Advanced Materials* **25**, 378-399 (2013).
18. Samanta, S. & Locklin, J. Formation of photochromic spiropyran polymer brushes via surface-initiated, ring-opening metathesis polymerization: reversible photocontrol of wetting behavior and solvent dependent morphology changes. *Langmuir* **24**, 9558-9565 (2008).
19. Davis, D. A. et al. Force-induced activation of covalent bonds in mechanoresponsive polymeric materials. *Nature* **459**, 68-72 (2009).
20. Kortekaas, L. & Browne, W. R. The evolution of spiropyran: fundamentals and progress of an extraordinarily versatile photochrome. *Chemical Society Reviews* **48**, 3406-3424 (2019).
21. Zhang, Q., Qu, D. H. & Tian, H. Photo-regulated supramolecular polymers: shining beyond disassembly and reassembly. *Advanced Optical Materials* **7**, 1900033 (2019).
22. Harada, J., Kawazoe, Y. & Ogawa, K. Photochromism of spiropyrans and spirooxazines in the solid state: low temperature enhances photocoloration. *Chemical Communications* **46**, 2593-2595 (2010).
23. He, X. J. et al. Reversible spiropyran-based chemosensor with pH-switches and application for bioimaging in living cells, *Pseudomonas aeruginosa* and zebrafish. *Dyes and Pigments* **180**, 108497 (2020).
24. Kim, D., Zhang, Z. Y. & Xu, K. Spectrally resolved super-resolution microscopy unveils multipath reaction pathways of single spiropyran molecules. *Journal of the American Chemical Society* **139**, 9447-9450 (2017).
25. Klajn, R. Spiropyran-based dynamic materials. *Chemical Society Reviews* **43**, 148-184 (2014).
26. Piech, M. et al. Patterned colloid assembly by grafted photochromic polymer layers. *Langmuir* **22**, 1379-1382 (2006).
27. Hu, C. L. et al. Visible light and temperature dual-responsive microgels by crosslinking of spiropyran modified prepolymers. *Journal of Colloid and Interface Science* **582**, 1075-1084 (2021).
28. Zhu, L. Y. et al. Reversibly photoswitchable dual-color fluorescent nanoparticles as new tools for live-cell imaging. *Journal of the American Chemical Society* **129**, 3524-3526 (2007).
29. Dou, Q. Q. et al. Dual-responsive reversible photo/thermogelling polymers exhibiting high modulus change. *Journal of Polymer Science Part A:Polymer Chemistry* **54**, 2837-2844 (2016).
30. Corredor, C. C. et al. Photochromic polymer composites for two-photon 3D optical data storage. *Chemistry of Materials* **19**, 5165-5173 (2007).
31. Rodŕıguez, A. et al. Optical control of an integrated interferometer using a photochromic polymer. *Applied Physics Letters* **79**, 461-463 (2001).
32. Arsenov, V. D., Marevtsev, V. S. & Cherkashin, M. I. Synthesis and photochromic properties of spiropyrane polymers with electron-donor substituents. *Polymer Science U. S. S. R* **27**, 2837-2843 (1985).
33. Berkovic, G., Krongauz, V. & Weiss, V. Spiropyrans and spirooxazines for memories and switches. *Chemical Reviews* **100**, 1741-1754 (2000).
34. Zhu, M. Q. et al. Reversible two-photon photoswitching and two-photon imaging of immunofunctionalized nanoparticles targeted to cancer cells. *Journal of the American Chemical Society* **133**, 365-372 (2011).
35. Liaros, N. et al. Elucidating complex triplet-state dynamics in the model system isopropylthioxanthone. *iScience* **25**, 103600 (2021).
36. Baldacchini, T. et al. Acrylic-based resin with favorable properties for three-dimensional two-photon polymerization. *Journal of Applied Physics* **95**, 6072-6076 (2004).
37. Schafer, K. J. et al. Two-photon absorption cross-sections of common photoinitiators. *Journal of Photochemistry and Photobiology A:Chemistry* **162**, 497-502 (2004).
38. Bongiovanni, R. et al. Perfluoropolyether polymers by UV curing: design, synthesis and characterization. *Polymer International* **61**, 65-73 (2012).
39. Andrzejewska, E. et al. Heteroaromatic thiols as co-initiators for type II photoinitiating systems based on camphorquinone and isopropylthioxanthone. *Macromolecules* **39**, 3777-3785 (2006).
40. Norrish type II reaction in Comprehensive Organic Name Reactions and Reagents, Wang, Z. R. , Hoboken: John Wiley & Sons, Ltd, 2010, 2067-2071.
41. Allen, N. S. Photoinitiators for UV and visible curing of coatings: mechanisms and properties. *Journal of Photochemistry and Photobiology A:Chemistry* **100**, 101-107 (1996).
42. Li, F. S. et al. Kinetic investigations on the UV-induced photopolymerization of nanocomposites by FTIR spectroscopy. *Journal of Applied Polymer Science* **99**, 1429-1436 (2006).
43. Fischer, E. & Hirshberg, Y. Formation of coloured forms of spiropyrans by low-temperature irradiation. *Journal of the Chemical Society* 4522-4524 (1952).
44. Pottier, E. et al. Effets de substituant, d'hétéroatome et de solvant sur les cinétiques de décoloration thermique et les spectres d'absorption de photomérocyanines en série spiro[indoline-oxazine]. *Helvetica Chimica Acta* **73**, 303-315 (1990).
45. Kellmann, A. et al. Photophysics and kinetics of two photochromic indolinospirooxazines and one indolinospironaphthopyran. *Journal of Photochemistry and Photobiology A:Chemistry* **49**, 63-73 (1989).
46. Baillet, G., Giusti, G. & Guglielmetti, R. Comparative photodegradation study between spiro[indoline-oxazine] and spiro[indoline-pyran] derivatives in solution. *Journal of Photochemistry and Photobiology A:Chemistry* **70**, 157-161 (1993).
47. Campredon, M. et al. ESR studies on some spiropyrans, spironaphthopyrans, and spirooxazines. *Journal de Chimie Physique* **91**, 1830-1836 (1994).